A Global Path Planning Strategy for a UGV from Aerial Elevation Maps for Disaster Response

D. C. Guastella, L. Cantelli, C. D. Melita and G. Muscato
Dipartimento di Ingegneria Elettrica Elettronica e Informatica, Università degli Studi di Catania, Catania, Italy

Keywords: Outdoor Environments, Rough Terrain, Unmanned Aerial Vehicle, Tracked Vehicle, Traversability, Path Planning.

Abstract: An approach for global path planning of an Unmanned Ground Vehicle (UGV) is proposed, including basic traversability analysis of the rough terrain to get through. The navigation capabilities of the UGV, in performing such analysis, are considered. The here proposed solution is organized into two following phases: first an aerial scan of the environment is executed by a UAV (Unmanned Aerial Vehicle) and the elevation map of the area is built; after that, a set of processing algorithms is applied to such surface model to derive a 2D costmap (whose costs are based on the prior traversability analysis) which is given as input of a D* path planner. The resulting path can be eventually delivered as a sequence of waypoints for a navigation controller on the field mobile platform.

1 INTRODUCTION

The need to have an autonomous robot moving across outdoor unstructured environments is not fully fulfilled by current state of the art in robotics, although it does represent a crucial point especially for disaster-response robots. Cooperative systems, namely unmanned aerial and ground vehicles working together, appear to show good performances for the above mentioned applications, thus justifying the increased interest on such approach in robotics research. A recent result is reported by Siegwart et al., (2015), where mechanical and structural aspects of a legged robot and a fixed-wing unmanned aerial vehicle are enhanced in order to improve their autonomy and stability in those harsh environments resulting from natural disasters. In some cases, the development of cooperative multi-robot systems has been encouraged by international robotics competitions, like EuRathlon (Schneider, Wildermuth and Wolf, 2015) or RoboCup Rescue (Kitano and Tadokoro, 2001), as in the case represented by ICARUS team, described by Marques et al. (2016), which was able to create cooperating robotic platforms in ground, air, and even maritime domains. It is apparent that there is the need to combine the contributions of heterogeneous platforms, especially when facing search and rescue scenarios. In addition, the difficulty of dealing with such risky environments is the severely limited possibility to perform non-destructive trials in the area of interest with the robotic platforms, in particular for UAVs. To address this issue some solutions have been proposed (Astuti et al., 2008).

The aim of the present work is to set up a procedure for the global path planning of an unmanned ground vehicle within an outdoor unstructured environment, taking into account the specific motion capabilities of the considered vehicle. The planning procedure is described as follows: starting from a Digital Elevation Model (DEM), which is built from the aerial photographic scan of the environment done by a multi-rotor, a traversability analysis on such terrain surface is performed, and finally an optimal path is computed, in terms of reducing the traversing cost. The path is planned with the D* algorithm (Stentz, 1994). The latter was preferred over other planning methods since it gives the possibility to include costs into the map and, moreover, it is optimized in replanning whenever such map of costs, i.e. the costmap, changes. The robotic platform considered in this work is the U-Go Robot, a tracked vehicle designed for rough terrain navigation (Bonaccorso et al., 2012), shown in Figure 1.

Guastella D., Cantelli L., Melita C. and Muscato G.
A Global Path Planning Strategy for a UGV from Aerial Elevation Maps for Disaster Response.
DOI: 10.5220/0006298303350342
In *Proceedings of the 9th International Conference on Agents and Artificial Intelligence (ICAART 2017)*, pages 335-342
ISBN: 978-989-758-219-6

The details about the digital elevation model reconstruction are given in Section 2, while Section 3 describes the first basic processing on such model, focusing on our case study. Then Section 4 reports the generation of the costmap, taking into account the traversability of the terrain with respect to our robotic platform. This point is the core and innovative part of the work. In Section 5 the results provided by the D* planner are shown, confirming the avoidance of those areas particularly hostile to be traversed. The final section includes a summary and an outlook for the current project.

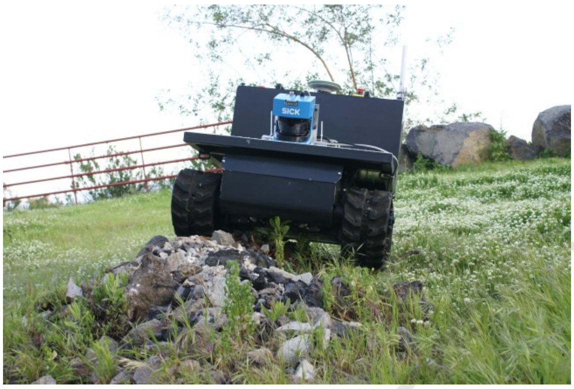

Figure 1: The U-Go Robot.

2 DEM RECONSTRUCTION

The starting data of the whole procedure is the DEM of the outdoor environment under inspection. This kind of model is typically referred to as 2.5D representation of the real world. The terrain surface to be represented is divided into cells and for each cell the highest altitude is stored, thus obtaining a matrix of altitudes. The result is a top view of the environment; therefore, the main drawback of the elevation maps consists of the impossibility to include overhanging structures or multiple height levels for one cell. However, they are still a good trade-off between computing power and representation accuracy in modeling outdoor areas. Each value inside the elevation matrix is pointed out with a couple of integers indicating its row and column. However, these heights have a relative distance in the real world, given by the resolution of the DEM, i.e. the size of the cells the terrain was divided into.

An innovative aspect lies in the DEM reconstruction. In particular, a scanning mission is previously performed by a quad-copter, during which the UAV autonomously covers the whole area to be reconstructed and takes regularly spaced pictures by means of a stabilized on-board camera. Then a commercial mapping software, Pix4Dmapper Pro, processes all the acquired pictures to recreate the 3D structure of the scanned terrain. Among different kind of processing outputs, the mapping software delivers the digital elevation model, along with its georeferencing information.

The environment considered in this case study is the external area of D.I.E.E.I. laboratories of the University of Catania. The resulting DEM is given in UTM coordinates (Universal Transverse of Mercator) with ellipsoidal heights (WGS84).

Furthermore, we focused our attention on a specific area within the outdoor environment, which resembles a landslide scenario, including areas with different slopes and level of navigation difficulties. The 3D textured mesh of this area is reported in Figure 2.

With an average flight altitude of 30 m and an on-board camera of 12.4 megapixels, the reconstructed digital elevation model has a resolution lower than 1 cm/cell (0.986 cm/cell) along both the North and East directions.

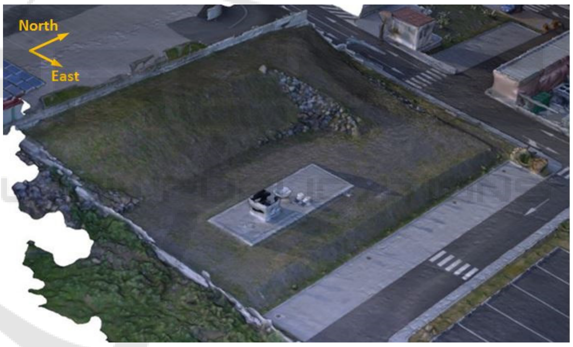

Figure 2: The 3D textured mesh of the landslide-like area recreated by the mapping software.

3 DEM PRE-PROCESSING

The overall processing of the elevation map is carried out in Matlab. Firstly the DEM, saved in geotiff format, is loaded in Matlab including its georeferencing information. At the same time the DEM is downsampled, thus obtaining a final spatial resolution of 9.86 cm/cell for the elevation map. This downsampling is performed to reduce the computing burden in the following processing steps and also for geometric considerations related to the robotic platform. In fact, the U-Go is a 75 cm long and 88 cm large tracked vehicle, with 18 cm wide rubber tracks. Therefore, working with height values spaced roughly every 10 cm is a sufficient approximation of the terrain surface over which the robot is supposed to move. Finally, from the whole DEM the region of interest is cropped, i.e. the landslide-like area. The final digital elevation model under study is a 451×337 matrix, representing an area of 44.47×33.23 m.

Since the idea was to generate a costmap including both maximum non-traversable slopes and height steps, a virtual wall was included into the digital elevation model by adding a fixed value to a rectangular shaped contour. Therefore, the final matrix considered for the global path planning is a slightly modified version of the original one, and in Figure 3 the resulting surface is depicted.

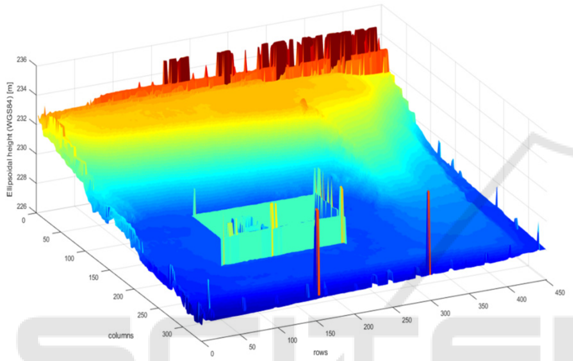

Figure 3: The reconstructed surface of the region of interest, after virtual wall insertion.

4 MAP GENERATION

Once defined the digital elevation model of the area under investigation, the following steps consist of processing such model in order to derive the costmap required by the path-planning algorithm.

4.1 U-Go Traversability Capabilities

A proper path planning cannot be conceived without taking into account the real motion actuation performed by the specific robotic platform, especially when the UGV is asked to autonomously cover hostile terrains and so a terrain traversability analysis must be included as well.

This task has been accomplished in literature in different manners. A remarkable example in this sense is shown by Santamaria-Navarro et al. (2015), which consists of application of learning models for traversable and non-traversable area classification. In that work the ground truth was made up of terrain appearance and geometry acquired by the vehicle while being teleoperated in the environment. A very similar method was also pursued by Silver, Bagnell, and Stentz (2010), where a skid-steering platform was firstly maneuvered by an expert, while learning a mapping between sensor data and path planning costs. Therefore, the vehicle usually learns in two senses: inferring its motion dexterity and/or determining the features of traversable and non-traversable terrain patches.

In our work, the U-Go was initially teleoperated over some testing areas, bringing its navigation performances to the limit. During these first experimental sessions a huge amount of proprioceptive data have been acquired; among them, the robot pose (roll, pitch and yaw angles of the vehicle) and the GPS coordinates.

As a first approach, two simple measures, in defining the U-Go motion capabilities, have been considered. From the inspection of pitch excursion, the minimum and maximum values recorded for this angle were respectively -29° and 32°; however nearly all the remaining values were within the [-25°, 25°] interval, whose limits are around the 80% of the two extreme values detected. Therefore, the *maximum traversable slope* for preventing the vehicle overturning is established at 25°, thus including a safety margin angle. Finally, the *maximum height step* that the U-Go is capable to climb was observed to be 15 cm.

4.2 Binary Occupancy Grids Generation

The georeferenced digital elevation model, descrybed in Section 3, is thus delivered to a Matlab processing function, which requires only maximum traversable slope and maximum climbable height, as inputs, and provides two binary occupancy grids, as outputs. The algorithm consists of the following main steps:

- Surface normals estimation in each point of the map;
- Height steps detection for each point of the map;
- Binary occupancy grids generation based on maximum slope and maximum climbable height.

Normals are used for the terrain slope assessment. The choice of using normals is justified by the possibility of quantitatively determining the slope exhibited by the terrain patch surrounding a given point. Using normals we essentially look at the z-component of these vectors. In fact, this component depends only on the cosine of the slope of the plane tangent to the surface in the considered point, with respect to the horizontal plane, as shown in Figure 4.

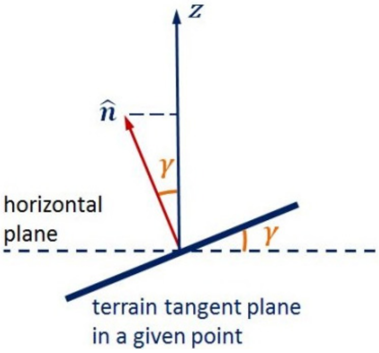

Figure 4: Normal z-component and tangent plane slope.

Normals estimation is performed using the implementation employed by Taylor, Nieto and Johnson (2015), which, however, is conceived to handle point clouds, i.e. xyz coordinates in the space. Therefore, in order to carry out this processing step, the DEM has to be previously converted into a point cloud.

The normals estimation algorithm computes a covariance matrix of a user-defined number of nearest neighbors of each query point and then performs a principal component analysis (PCA). The eigenvector associated to the minimum eigenvalue gives the best normal direction estimate of the tangent plane in the query point (Rusu, 2009). Furthermore, this PCA-based technique requires the indication of a point of view, to determine the normal vectors orientations, consistently with the surface. In our case a point of view in the center of the surface, with a high altitude value, was chosen, in order to have nearly all normals pointing in the positive direction of the z-axis, thus allowing us to deal with positive z-components.

Normals estimation has been carried out on a smoothed version of the DEM, which has been obtained by applying a Gaussian convolutional filter over the matrix. The standard deviation of the Gaussian filter establishes the kernel size of the convolutional filter. In our case a standard deviation equal to 2 is chosen, leading to a kernel size equal to $2 \cdot \lceil 2\sigma \rceil + 1$=9. This particular value has been chosen since it has shown to improve the quality of the normal estimation results, generating a less noisy output, without compromising too much the final resolution, thinking of the robotic platform size. Then the smoothed matrix has been converted into a point cloud and normals for each point have been computed. In Figure 5 a sample graphical result is shown.

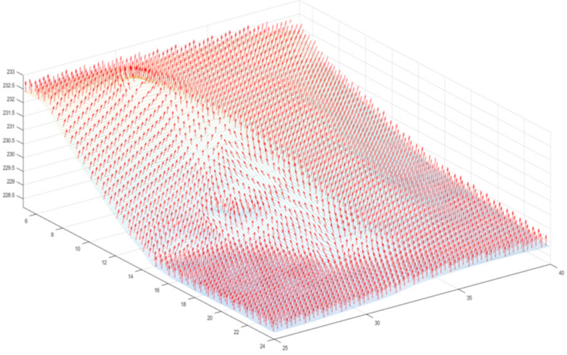

Figure 5: Detail of normals estimated over the terrain.

The z-components of these normals are rearranged as a matrix, in order to have a one-to-one matching with the original DEM. This matrix of z-components is finally compared with a threshold, which is the cosine of the slope above which the terrain is non-traversable, i.e. 25° (see Figure 4). In this manner the first binary occupancy grid is generated. To exclude areas all surrounded by non-traversable points (and then unreachable), holes in the binary image are immediately filled.

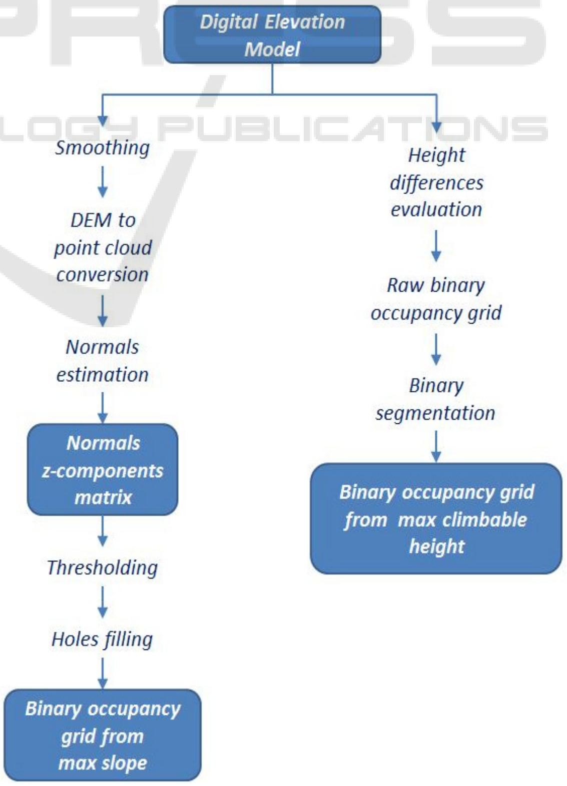
Digital Elevation Model
Smoothing
DEM to point cloud conversion
Normals estimation
Normals z-components matrix
Thresholding
Holes filling
Binary occupancy grid from max slope
Height differences evaluation
Raw binary occupancy grid
Binary segmentation
Binary occupancy grid from max climbable height

Figure 6: Scheme of the processing phases of the two occupancy grids generation.

Then the Matlab processing function builds the second binary occupancy grid, which looks for discontinuities in the height values exceeding a maximum threshold (namely steps or walls). The method to realize this binary occupancy grid is straightforward: for each element of the DEM we compute all the absolute differences between the element value and the values of its eight adjacent surrounding elements; if at least one of these differences is above the threshold, the cell is marked as an obstacle. It is apparent that such solution does not hold for the DEM boundaries; therefore, they are discarded in the following steps. Finally, a binary segmentation is performed on the occupancy grid: this allows to exclude unreachable isolated areas (all surrounded by non-traversable cells) and, more importantly, to make the shapes of these real obstacles stand out, rather than simply filling holes as in the previous case. In Figure 6 a sketch of the processing steps carried out within the Matlab function is reported.

4.3 Costmap

The last map to create is the global costmap for the D* path planner (Stentz, 1994), depending on which the algorithm identifies the optimal path, i.e. the route with lower cumulative cost. The costs within this map are generically values greater than zero; in the implementation that we use, included in the *robotics toolbox* v. 9.10 (Corke, 2011), the algorithm works in particular with costs greater than one. In any case obstacles are mapped with infinite values.

A second Matlab function is in charge of generating this costmap. Firstly a global binary occupancy grid is built by simply merging the two occupancy grids described in the previous section (i.e. taking the union of their non-traversable cells). Note that in this binary map obstacles and free cells are respectively represented with one and zero, but in the final costmap they will be respectively remapped with infinity and one. Furthermore, the costs of non-obstacle cells are derived as explained below.

To prevent the path planner from choosing cells too close to those marked as obstacles, the costs of all these cells are increased by dilating obstacle areas, applying a large-sized Gaussian kernel to the binary occupancy grid and multiplying the resulting matrix by a magnifying factor. In this way only costs of the desired cells are increased, since the ones farther from obstacles still have a zero value after the dilation, which obviously is not affected by the multiplication. A second contribution included in non-obstacle cells costs is the slope. In fact, although all cells with slope higher than 25° are already marked as obstacles, it is still preferable to avoid to have the robot traversing terrain patches with high slope and, in general, to move along a path with as lower steepness as possible, both for safety and energy efficiency reasons. Therefore, starting from the matrix of normals z-components (described in the previous subsection), we associate higher costs to those cells with inclination close to 25° (i.e. whose values in the matrix is close to *cos(25°)*), and costs close to 1 (i.e. traversable cells in the D* costmap) to those cells with slope close to 0° (i.e. whose value in the matrix is close to 1).

A further feature, which was considered in the first instance of the costmap derivation, was the terrain unevenness. In fact, PCA analysis performed on the point cloud allows to acquire information on both the terrain irregularity and the terrain normals at the same time, since they are respectively related to the smallest eigenvalue and the corresponding eigenvector of the covariance matrix. However, this kind of information was not included in the final costmap since, in our case study, it appeared to introduce only noise in the planned path, without any remarkable quality increase, since highly irregular areas have been already marked as obstacles.

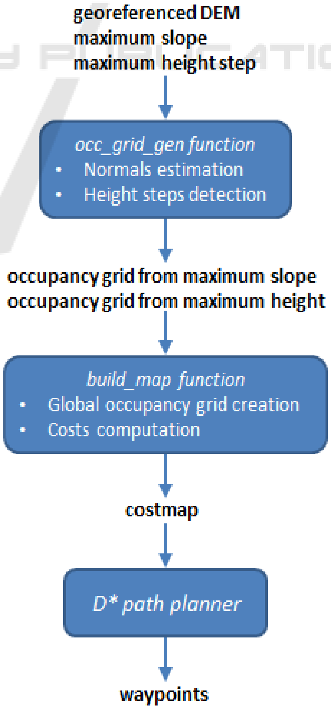

Figure 7: Scheme of the overall procedure, starting from the digital elevation model up to waypoints generation.

Eventually, to obtain the global costmap for the D* algorithm, all matrices are merged together: the global occupancy grid, including cells with infinite costs (i.e. obstacles), with the two matrices of costs for obstacle-closeness and costs for cells slopes.

Once provided the costmap, the path planner can compute the optimal route, which is converted into a sequence of waypoints. In Figure 7 a summarizing scheme of the overall workflow is shown.

5 RESULTS AND SIMULATIONS

Two sample paths have been computed, from two different couples of starting and final points, delivering them to the D* planner. In Figure 8 these paths are shown: both the starting points, and the final points (indicated with blue dots) are chosen to make the vehicle reaching the upper part of the area starting from the lower part and vice-versa. The lighter grey shades are those cells of the costmap with higher cost, while red areas are absolutely non-traversable zones (i.e. those marked as obstacles in the global binary occupancy grid described in the previous subsection).

Then these trajectories are converted into UTM and longitude/latitude coordinates, in order to be provided as references to the waypoint navigation controller on board of the tracked vehicle. A Matlab script running on a laptop, acting as a control base station, is employed to interact with the vehicle by means of the ROS (Robot Operating System) communication middleware, thanks to the Robotics System Toolbox, which provides an interface between Matlab and the ROS network.

In Figure 9 the red tracks represent the 3D reconstructions of the paths over the terrain surface.

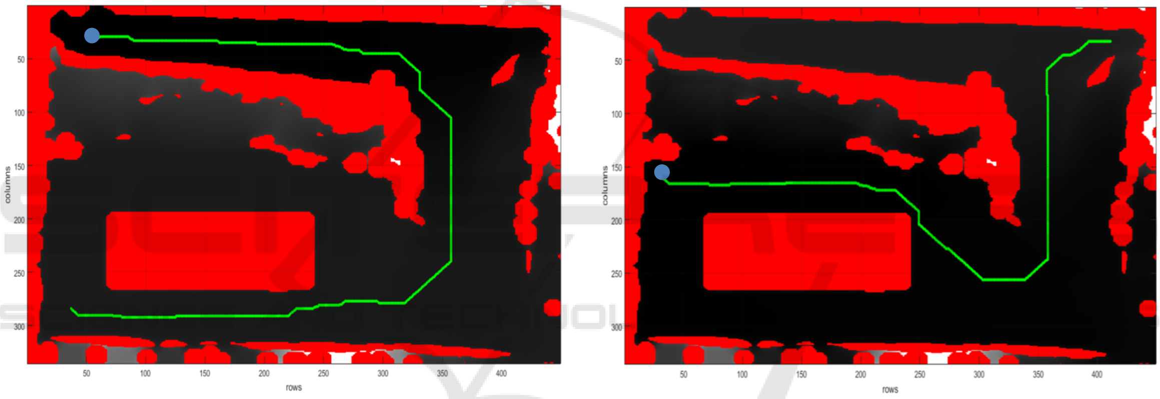

a)

b)

Figure 8: Examples of computed paths: a) path #1 (path length: 75.62 m); b) path #2 (path length: 56.20 m).

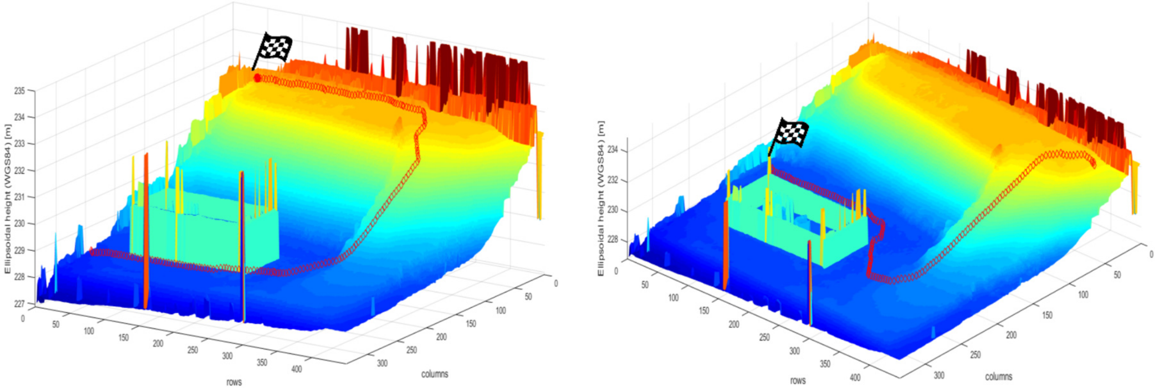

a)

b)

Figure 9: Track of the vehicle over the terrain: a) path #1; b) path #2.

6 CONCLUSIONS AND FUTURE DEVELOPMENTS

The work presented in this paper is an end-to-end procedure to perform a global path planning for a UGV, starting from a digital elevation model built from an aerial photographic acquisition, carried out by a UAV, of the field over which the ground vehicle has to move. This approach is particularly relevant for search and rescue scenarios, where the environment to cope with is strongly unstructured, heterogeneous and not known a priori.

Thanks to the simple kind of analysis performed on the surface model, the procedure allows to obtain a traversable path in a very brief time interval, avoiding dangerous steep slopes and steps. In this manner, the vehicle is capable to start operating over the area to be rescued, while more task-specific missions can be planned in a longer time. Moreover, the solution here presented can constitute a good background to be integrated with a local obstacle avoidance controller, supported by the optimized replanning method of the D* algorithm.

A future development could be to move to a full 3D representation of the outdoor environment, for instance by using octomaps (Hornung et al., 2013), or dense point clouds. In this manner overhanging structures, which are quite often present in disaster areas, and terrain roughness analysis could be included, thus allowing to find more traversable paths. Moreover, some solutions to obtain the environment reconstruction in real-time could be introduced such as the one reported in Pizzoli, Forster and Scaramuzza (2014).

However, the work here reported, even if much simpler, could be smartly integrated into a more complex solution to reduce computing burden, for instance, focusing only on those traversable terrain areas identified by the costmap generation process.

Another point to be enhanced is the overall system robustness. The communication system should not only rely on the ROS framework, which is more suitable for reliable communication network. The capability of moving also in GPS-denied environments should be included, by resorting to SLAM or Visual Odometry, as done by Siegwart et al. (2015) and Weiss, Scaramuzza and Siegwart (2011), thus avoiding to trust only on GPS information, not always available in disaster areas. Matlab and ROS have been used in this prototyping phase to study the first results of the procedure; however, everything should be embedded in a companion PC on-board to the vehicle, thus making the whole planning strategy much less “manual”, once platform-dependent parameters have been properly tuned.

Finally, while computing the path, the orientation of the platform with respect to the terrain was not considered. This would result in too much of a conservative representation of the area, in terms of traversability, because for each terrain cell only maximum slope is considered. Therefore a first integration will be to use a modified version of the D* planner and to consider also the physical size of the platform and not just schematize it as a point mass.

ACKNOWLEDGEMENTS

This work was carried-out in the framework of the CLARA PON project. The Project CLARA (CLoud plAtform and smart underground imaging for natural Risk Assessment) is funded by MIUR under the program PON R&C SCN_00451.

REFERENCES

Siegwart, R., Hutter, M., Oettershagen, P., Burri, M., Gilitschenski, I., Galceran, E., Nieto, J., 2015. Legged and flying robots for disaster response. In *World Engineering Conference and Convention 2015 (WECC2015)*.

Schneider, F.E., Wildermuth, D., Wolf, H. L., 2015. ELROB and EURATHLON: improving search & rescue robotics through real-world robot competitions. In *IEEE 10th International Workshop on Robot Motion and Control (RoMoCo)*.

Kitano, H., Tadokoro, S., 2001. Robocup rescue: a grand challenge for multiagent and intelligent systems. In *AI magazine, vol. 22(1)*.

Marques, M. M., Parreira, R., Lobo, V. et al., 2016. Use of multi-domain robots in search and rescue operations - contributions of the ICARUS team to the euRathlon 2015 challenge. In *Oceans 2016*.

Astuti, G., Longo, D., Melita, C. D., Muscato, G., Orlando A., 2008. HIL tuning of UAV for exploration of risky environments. In *International Journal on Advanced Robotic Systems, Vol. 5(4)*.

Stentz, A., 1994. The D* algorithm for real-time planning of optimal traverses. *Tech. Rep. CMU-RI-TR-94-37, The Robotics Institute, Carnegie-Mellon University*.

Bonaccorso, F., Longo, D., Muscato, G., 2012. The U-Go Robot, a multifunction rough terrain outdoor tracked vehicle. In *Proceedings of the 2012 World Automation Congress WAC2012*.

Santamaria-Navarro, A., Teniente, E. H., Morta, M., Andrade-Cetto, J., 2015. Terrain classification in complex three-dimensional outdoor environments. In *Journal of Field Robotics, vol. 32(1), pp. 42-60*.

Silver, D., Bagnell, J. A., Stentz, A., 2010. Learning from demonstration for autonomous navigation in complex unstructured terrain. In *The International Journal of Robotics Research vol. 29(12), pp.1565-1592*.

Taylor, Z., Nieto, J., Johnson, D., 2015. Multi□modal sensor calibration using a gradient orientation measure. In *Journal of Field Robotics, vol. 32(5), pp. 675-695*.

Rusu, R. B., 2009. *Semantic 3D object maps for everyday manipulation in human living environments*. PhD thesis, Computer Science department, Technische Universität Müchen, Germany.

Corke, P. I., 2011. *Robotics, Vision & Control*, Springer.

Hornung, A., Wurm, K. M., Bennewitz, M., Stachniss, C., Burgard, W., 2013. OctoMap: an efficient probabilistic 3D mapping framework based on octrees. In *Autonomous Robots, vol. 34(3), pp. 189-206*.

Pizzoli, M., Forster, C., Scaramuzza, D., 2014. REMODE: probabilistic, monocular dense reconstruction in real time. In *IEEE International Conference on Robotics and Automation (ICRA), pp. 2609-2616*.

Weiss, S., Scaramuzza, D., Siegwart, R., 2011. Monocular-slambased navigation for autonomous micro helicopters in gps-denied environments. In *Journal of Field Robotics, vol. 28(6), pp. 854-874*.